



3-Phase grid-connected building integrated photovoltaic system with reactive power control capability



Mohan Lal Kolhe, PhD Professor ^{a, b}, M.J.M.A. Rasul ^{a, *}

^a Dept. of Engineering Sciences, Faculty of Engineering and Science, University of Agder (UiA), N-4898, Grimstad, Norway

^b Smart Grid and Renewable Energy, Faculty of Engineering and Science, University of Agder, N-4879, Grimstad, Norway

ARTICLE INFO

Article history:

Received 10 June 2019

Received in revised form

10 March 2020

Accepted 12 March 2020

Available online 16 March 2020

Keywords:

Grid-connected PV system

Voltage source inverter

Reactive power control

Voltage regulation

ABSTRACT

Recently, a tendency in the growing of grid-connected building integrated photovoltaic (BIPV) systems has been noticed in most countries. Hence, high penetration of PV power into the system network can be observed in many points in the network. This may cause severe problems on the distribution network due to the intermittent nature of PV systems. As a feasible solution, the reactive power capability of voltage source inverter in PV systems can be employed rather than approaching expensive grid infrastructures in the distribution network. The purpose of this study is to implement a 3-phase grid-connected (BIPV) system with reactive power control to regulate the system voltage and improve the system power factor. Subsequent to this, a specific system model has been designed and developed in MATLAB Simulink application. The selection of PV system specifications is based on practical system implementation. The inverter control system along with the reactive power control has been developed for the proper system operation at different system conditions to reduce the var compensation on the utility grid. Better system accuracy of the developed system model has been found by validating with real system data. The overall system performance has indicated that the effective utilization of reactive power control of a grid-connected PV system yields to a stable, reliable and cost-effective system network operation which reduces the heavy burden on the utility grid to control the PV system effects.

© 2020 Elsevier Ltd. All rights reserved.

1. Introduction

Presently, a tendency in the rapid growth of energy has been noticed in the world. Hence in most of the countries, renewable energy resources (RES) have been utilized in electricity production. The main available RESs are hydroelectric, biomass, photovoltaic, wind, geothermal and tidal systems and also called the alternative source of energy which can be used again and again. Consequently, this increase in renewable energy generation systems combined with power electronic systems, the microgrid concept has been developed. The capability of operating in an uninterruptible way either grid-connected or islanding mode is the main benefit of a microgrid.

Integrating RESs such as wind and solar, into the utility grid at the distribution level, is a trending fact. These distributed energy

resources (DERs) supply power directly to the grid via power electronic converters where the final stage is a DC-AC inverter between the DERs and the grid. In recent years, Photovoltaic (PV) system has been the fastest growing power generation system worldwide, has a total capacity of 228 GW at the end 2015 [1]. Generally, the available types of PV systems are residential scale, commercial scale and utility scale in which capacities range from few kilowatts to hundreds of megawatts.

These PV systems inject real power to the grid via at many points in the distribution network. Since this is an effective solution for rapid growing energy demand, but this will bring adverse consequences on the entire distribution network. This is because of the intermittent behavior of the PV energy which accordingly have an impact on the availability, reliability, and quality of the distributed grid. Due to this intermittent nature and cumulative real power injections at different points, it is a very much complex process of making reliable estimations of the power circulations throughout the distribution network employing a few readings at a few different locations. In case of high PV production level, the whole power system will be out of control and there is a potential

* Corresponding author. Ocean University of Sri Lanka, Crow Island, Mattakuliya, Colombo 15, Sri Lanka.

E-mail addresses: mohan.l.kolhe@uia.no (M.L. Kolhe), ashikmar@gmail.com (M.J.M.A. Rasul).

risk of significant reverse power circulation, and accordingly causing unacceptable voltage hike in the network voltage [2–4].

To overcome this abnormal voltage over-limits situations, the expensive grid infrastructures such as under-load tap changing transformers (ULTC), step voltage regulators (SVR), and fixed and switchable capacitors (FC and SC), can be deployed or the reactive power control ability of voltage source inverter (VSI) in PV systems can be utilized for injecting or absorbing reactive power for voltage compensation as an ancillary service [5,6]. The advantages of utilizing PV inverters over expensive grid infrastructures are the capability of providing continuous variable reactive power which enables to manage the voltage more closely, and inverter quick response in comparison with switched capacitors [7].

Previously the IEEE Standard for Interconnecting Distributed Resources with Electric Power Systems (IEEE Std 1547, 2003) [8] states that the DERs are not permitted to regulate the voltage at the point of common coupling (PCC). Due to some technical problems arise with high PV penetration level after rapid growth in PV energy production, the amendment IEEE Std 1547a-2014 [9] unleashes the restrictions that the DERs are allowed to actively engage in regulating the grid voltage by making alterations to the active and reactive power productions of the DERs coupled with mutual agreements with the distribution grid operators and the DERs.

Hence, the PV inverters can be utilized as the fast acting local var compensators in the areas with significant levels of PV penetration, providing reactive power absorbed by local loads as measured at their point of common coupling (PCC) and subsequently help to enhance the power factor (PF) at PCC. This will assist to attenuate the voltage regulation problems along with the PF improvement while enhancing the grid stability and maximizing the power transmission capability by reducing transmission loss. In the meantime, this will be a significant economic benefit for consumers to avoid the cost of the equipment required to control the PF.

With the rapid growth in the penetration level of PV power on the distribution system, voltage fluctuations issues can be arisen around the location of the interconnection of PV systems due to the real power injection of PV systems. The reactive power control functionality of PV inverter has been utilized to support the voltage regulation at the distribution level. In recent years, most of the researches have been focused on the reactive power control strategies for grid-connected PV inverters for active contribution on the voltage regulation.

Different techniques have been discussed for the voltage support, based on the reactive power compensation of the PV inverter in literature. Those can be grouped as fixed PF (fixed $\cos\phi$), PF as a function of the active power ($\cos\phi(P)$) fed into the network, fixed reactive power (fixed Q), reactive power as a function of the voltage at the point of common coupling ($Q(V)$) [10,11] and reactive power as a function the active power ($Q(P)$) [12]. Besides these technologies, several studies have been presented based on the reactive power control along with the active power curtailment for voltage regulation problem [13–16].

Reference [17] presented a three-phase grid interactive PV inverter with reactive power ability to support the grid voltage regulation. The proposed system was enabled to operate in unity PF, variable PF, and zero PF to meet the grid requirements. In [18], an adaptive decentralized voltage restriction control by the autonomous reactive power control of grid-connected PV inverters was presented and tested on different LV grids to reduce the necessity of additional grid reinforcement measures. The proposed strategy based on the V-Q characteristics with a dead band where the reactive power injection or consumption by the inverter was initialized when the voltage limitations exceed. The work in [19] addressed a reactive power control ($Q(V)$) relying on voltage for an inverter with a PF of 0.9 for compensating the voltage rise due to

the PV power feed in an MV network located in Belgium.

A power control approach based on the single-phase active-reactive power theory which was controlled by system conditions and specific demands from both system operators and customers was presented in [20] to enable the PV inverters to perform the multi-functional ancillary services such as “low voltage ride through (LVRT), reactive power compensation and reliability-oriented thermal management” on PV inverters. The prescribed power control strategy was developed and utilized under the limitation of the PV inverter ratings. Similarly, in [21], an inverter control strategy was based on the PQ theory which facilitates to produce the active power and compensate the reactive power of the loads during daytime while only compensating the reactive power of the loads during night time.

Utilizing analysis of voltage sensitivity by setting a location dependent PF to each PV inverter units for the grid voltage support control was presented in [22] as a decentralized reactive power. In this work, the combination of aforementioned strategies, $\cos\phi(P)$ and $Q(V)$, was employed to avoid the unnecessary absorption or injection of reactive power during over-voltage conditions. A similar approach using the voltage sensitivity analysis was discussed in [23] for the reactive power control of the PV systems, to attenuate the voltage fluctuations due to the active power variations of the PV systems. The effect on the inverter efficiency was discussed for three different modes of reactive power control to investigate the inverter performance.

In [24], an inverter reactive power injection control was designed, based on the volt/var control as a “radial optimal power flow (OPF) problem”, subjected to the constraints of voltage and PV inverter reactive power limit where the objective was to reduce the line losses, the energy consumptions and the cost of inverter losses when not operating at unity PF. Reference [25] discussed a method, based on the absorption and injection of uneven reactive power by three-phase PV inverters, to avoid the voltage unbalance due to the high penetration of single-phase inverters in the LV grid. In this proposed method, the average values of the phase voltages at the PCC of the PV inverters were employed as the references for the balancing algorithm for controlling each phase independently to achieve uneven compensation and also reducing the over-voltage conditions.

An active power dependent (APD) ($Q(P)$) voltage regulation method was proposed in [26] in which the required reactive power to manage the voltage was calculated in terms of the penetrated real power of a PV system. In this proposed method, an active power threshold, based on the investigation of the “voltage sensitivity matrix”, was employed as a start point above which the PV system was ready to consume reactive power to regulate the voltage. Reference [27] discussed an active power dependent reactive power compensation method without utilizing a threshold into the system where the aim was to optimally dispatch the inverter reactive power while maintaining the voltage within an admissible range and minimizing the resistive losses over the entire network. An “optimal inverter dispatch (OID)” framework was proposed in [28] where the task was to determine both the real and reactive power set points of the PV inverter so that to optimize the network operation by minimizing the power losses while assuring the voltage regulation and adhering to other electrical network constraints. The proposed OID framework increased the adaptability over the volt/var support and the active power restriction, by invoking a combination control of active and reactive powers generated by the PV inverters.

The work in [29] proposed a control strategy for the PV inverters to enhance the operational performance of the unbalanced four-wire distribution networks with high PV production, based on the optimal generation capability of reactive power and the real

power restriction. An optimization problem with the objectives of voltage magnitude, network losses, PV production and active power restriction costs was addressed in previous work to find the optimum control values. In [30], a combination of droop-based inverter reactive power control technique with the active power curtailment (APC) technique was addressed to maintain the local voltage profile within pre-defined limits, in the case of large-scale PV implementation in a specific location. In this approach, the APC was employed only to improve the inductive reactive power generation at the maximum PV generation time.

Based on the literature reviews, the inverter reactive power compensation on both voltage regulation and PF improvement on building integrated PV (BIPV) systems have not been considered together. Hence, this research work is mostly focused on enabling reactive power control of a grid-connected BIPV system for automatic voltage regulation and PF improvement based on PCC load conditions. The reactive power control system is mainly subjected to the inverter capacity with the instantaneous PV power without any active power curtailment injecting to the grid. Most BIPV systems operate at unity PF where the systems inject only real power to the grid. This may have the effect of lowering the PF at the PCC of a lagging power system. Fig. 1 indicates an example of this effect. The power relationship of the relevant load is given as S1 at a PF of 0.95 (18.15°) lagging. If a PV system that injects only active power at a unity PF, is installed at the PCC, the PF of the power combination S2 that is seen at the PCC will reduce to 0.75 (41.41°) lagging. Even though for a small-scale residential PV system, this cannot be neglected. Hence, it would be financially favourable to the electrical power system as well as to the consumers if the PV systems could operate with the facility of reactive power compensation at a local level.

2. Modeling of PV system components

In grid-connected PV systems, the power electronic devices are used to connect the PV model into the grid because of its stochastic nature. The different PV system configurations are concerned to connect the PV modules into the grid.

Usually, the configurations can be divided into two categories, as illustrated in Fig. 2, such as the PV inverters with DC/DC converter (Double-Stage) and the PV inverters without DC/DC converter (Single-Stage) [31,32].

The double-stage PV system with a boost converter is used for this research study for boosting the PV voltage to a higher level. In this case, the maximum power point tracking (MPPT) is controlled by the boost DC-DC converter. The boost DC-DC converter is connected to the grid through a DC/AC inverter, which takes care of the grid current control and the grid synchronization [33].

Fig. 3 represents the overall system configuration diagram of the grid-connected BIPV system. The system components are connected by the solid lines to represent the power flow while the

control systems are connected by the dotted lines to represent the signal flow.

2.1. PV array model

The PV array block which is included in the MATLAB Simulink library is used as the PV array model. The PV array block enables to select the inbuilt preset PV model from the National Renewable Energy Laboratory (NREL) System Advisor Model. The PV array model is implemented as strings of the module connected in parallel. The string module is built up with series connected modules. As the main inputs of the PV array module, the solar intensity and the cell temperature values are considered. The SunPower PV panel is considered in the modeling and the PV model specifications are given in Table 1.

2.2. DC-DC boost converter model with controller model

To ensure the optimal operating condition of the PV system, it should produce the maximum power all the time under specific meteorological conditions. The PV output power along with the maximum power varies with solar radiation, ambient temperature and cell temperature as shown in Fig. 4. Hence, this is a prominent factor to track the maximum power point of the PV array under different operating conditions. Consequently, the maximum power point tracking (MPPT) control algorithm is utilized to provide the maximum continuous power from the PV array based on the variation in the irradiation and the temperature.

In the past few years, many MPPT techniques have been developed. The Perturb and Observe (P&O) method and the Incremental Conductance (IC) algorithms are the most commonly applied algorithms as the simple structure [34]. A major drawback of P&O algorithm is failed to response sudden changes in solar irradiance and it continues the process as a change in MPP due to perturbation. This yields to end up calculating the wrong MPP [34]. The incremental conductance algorithm can be used to overcome the problem occurs in the P&O algorithm [34]. This algorithm is based on the slope of the PV array power curve. The basic equation of this algorithm is given in equation (01) [35]. The graphical interpretation of the incremental conductance algorithm is represented in Fig. 5.

$$\begin{cases} \frac{dP}{dV} > 0; & v < V_{mpp} \\ \frac{dP}{dV} = 0; & v = V_{mpp} \\ \frac{dP}{dV} < 0; & v > V_{mpp} \end{cases} \quad (1)$$

As the main function of the boost converter, the duty cycle of the converter is varied under all conditions in order to efficiently track the MPP of the PV array. The DC bus voltage of the system is kept at 800 V. When PV array is in MPP operating condition under 1000 W/m² of solar irradiance and 25 °C of cell temperature, its output voltage is 273.1 V. Hence, a DC-DC boost converter is deployed to step up the PV array output voltage. The model of the boost converter is shown in Fig. 6. The IGBT is utilized as the power switching device in the converter.

The gate pulses for the IGBT are generated by the boost converter controller accordingly by varying the duty ratio in order to track the MPP of the PV panel. The incremental conductance algorithm is utilized to follow the MPP voltage of the PV panel and the duty cycle is continuously changed accordingly to produce the pulses for the boost converter. The model of the boost converter

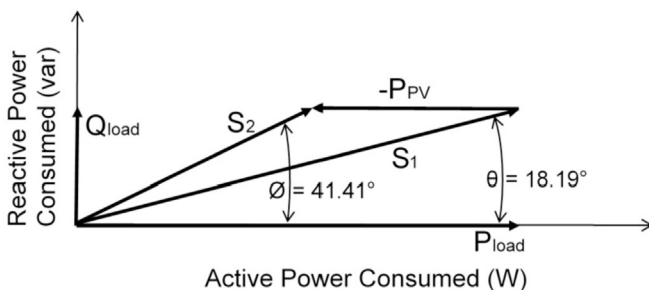


Fig. 1. Active and reactive power relationship for a unity power factor PV system.

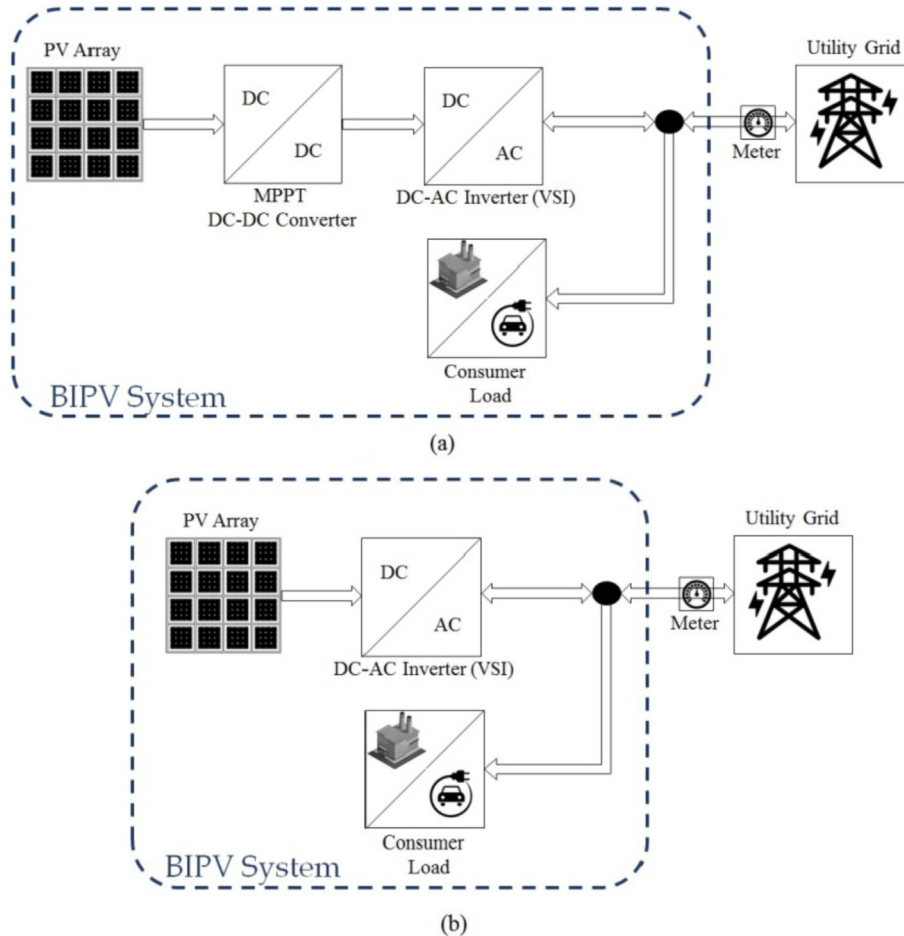


Fig. 2. Grid-connected BIPV system configurations (a) Double-stage (b) Single stage.

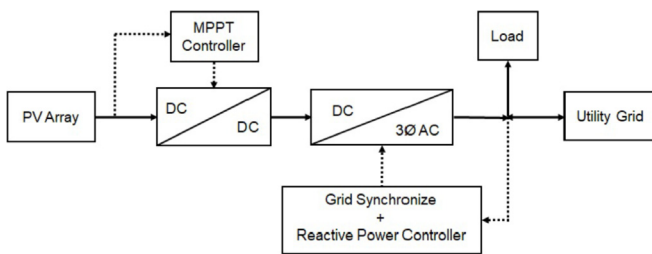


Fig. 3. Overall system configuration diagram of the grid-connected BIPV system.

controller with MPPT function is illustrated in Fig. 7. The initial duty cycle is set as 0.5 in the controller.

2.3. Voltage source inverter (VSI) model with controller model

In grid-connected PV systems, the main task of the DC-AC inverter or VSI is to convert the PV array DC power to the AC power with grid synchronization, while managing the boost converter DC output voltage in double-stage configurations. A three-phase inverter which is used in a grid-connected PV system is voltage source inverter (VSI) type equipped with power switching devices (Insulated gate bipolar transistors (IGBT), Gate turn of thyristor

Table 1
PV module specifications (SUNPOWER SPR-305E-WHT-U).

| PV Module | |
|--------------------------------|---------|
| Maximum Power (W) | 305.226 |
| Open Circuit Voltage (V) | 64.2 |
| Short Circuit Current (A) | 5.96 |
| Voltage at MPP (V) | 54.7 |
| Current at MPP (A) | 5.58 |
| Cells per module | 96 |
| Modules in series (PV Array) | 5 |
| Modules in parallel (PV Array) | 5 |
| Maximum Power (kW) (PV Array) | 7.63 |

(GTO) or Metal-Oxide semiconductor field-effect transistor (MOSFET)).

In this research study, the inverter offers the reactive power compensation service as an additional service. Hence, the two-quadrant operation of the VSI is available as shown in Fig. 8.

The selected inverter capacity of 9.5 kVA is larger than the maximum PV capacity of 7.63 kW where the inverter maximum operating PF is 0.8 at the maximum PV capacity. Consequently, the inverter has the ability to produce reactive power at the maximum PV system operation as indicated in Fig. 8. The P-Q relationship of the inverter is given in equation (2).

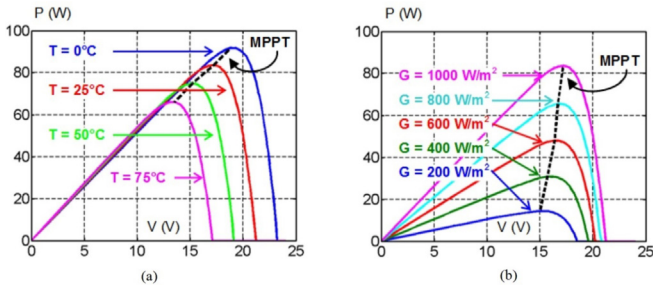


Fig. 4. P–V characteristic curve of a PV module (a) Effect of temperature changes (b) Effect of solar irradiance changes.

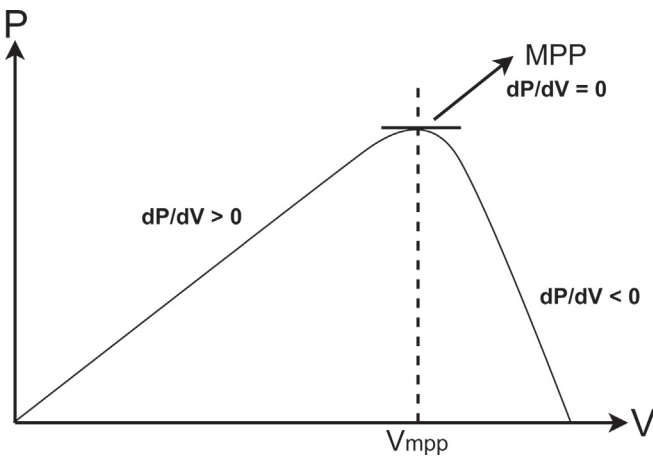


Fig. 5. Illustration of the incremental conductance algorithm on the P–V curve of a PV array.

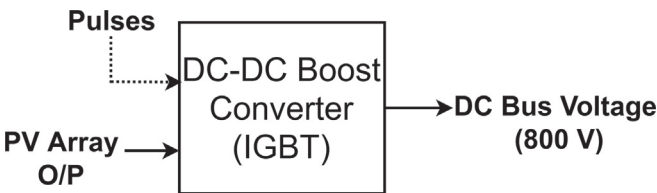


Fig. 6. DC-DC boost converter model.

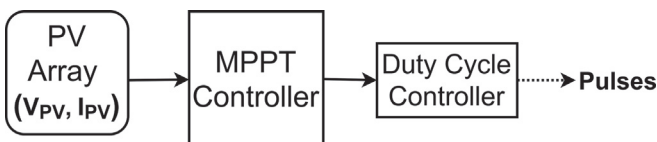


Fig. 7. MPPT controller model.

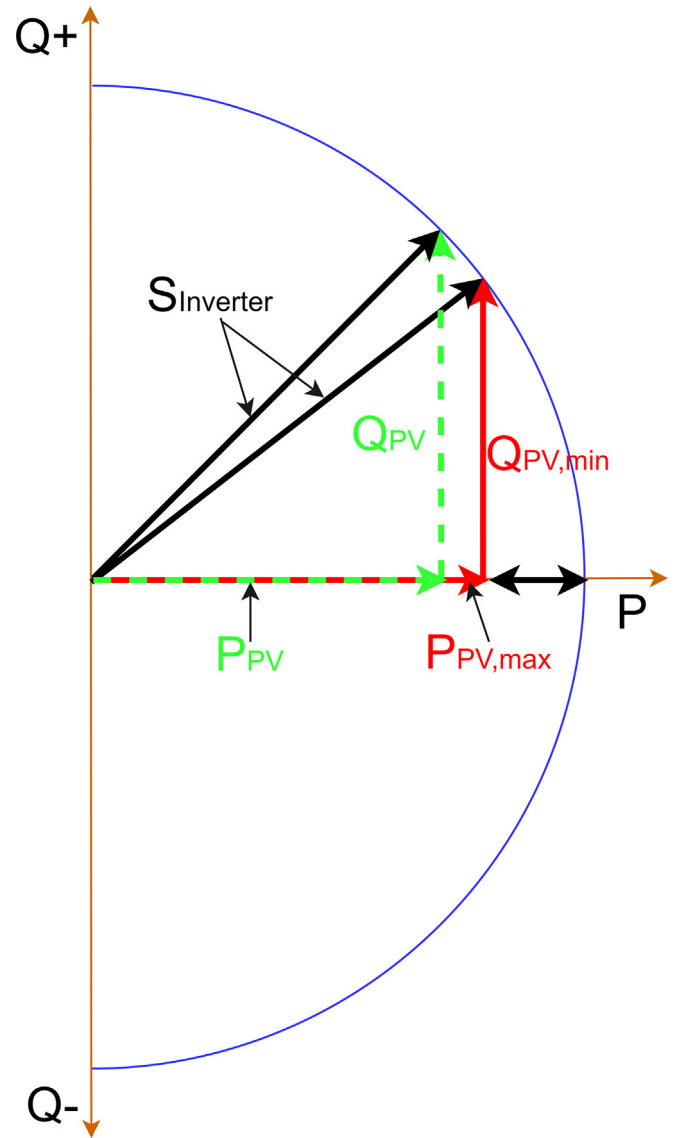


Fig. 8. VSI 2-quadrant operation.

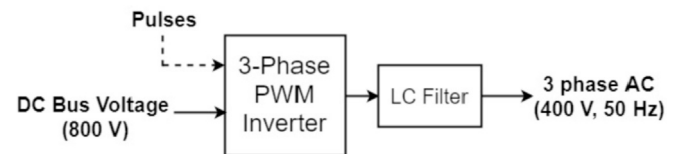


Fig. 9. VSI model.

$$Q = \begin{cases} S \times \sin \left[\cos^{-1} \left(\frac{P_{PV,max}}{S} \right) \right]; & P = P_{PV,max} \\ \sqrt{S^2 - P^2}; & P = P_{PV,max} \end{cases} \quad (2)$$

where S is the Inverter capacity, P is the instantaneous PV Power of the PV array, $P_{PV,max}$ is the maximum PV power of the PV array and Q is the reactive power of the inverter.

A three phase PWM generator is used to drive the IGBTs in the inverter. The VSI sets the input DC voltage at 800 V and transforms into a three-phase AC voltage of 400 Vrms with a frequency of

50 Hz. The harmonics caused by the inverter is filtered out by deploying an LC filter. The VSI model is depicted in Fig. 9.

The inverter controller system shown in Fig. 10 is responsible for generating the PWM signals in the way to synchronize the PV system with the grid. The control system consists of a DC voltage regulator, a phase lockup loop (PLL) block, a current controller block, and a PWM signal generation block. The PLL converts the three-phase time varying system into DC system components ($[V_d, V_q]$ are voltage components and $[I_d, I_q]$ are current components) and measures these DC components along with the phase angle of the grid which are to be used for the grid synchronization purpose.

The DC voltage regulator generates the I_d current reference which is to produce the instantaneous PV power from the inverter as an active power. The I_q current reference is generated from reactive power controller to maintain the inverter output voltage within the range of $\pm 5\%$ of 400 V by producing relevant reactive power from the inverter. The current controller output gives the references of V_d and V_q based on the I_d and I_q references with the measured I_d, I_q and V_d, V_q values from the PLL. The PWM signal is generated based on the three modulating signals which are generated from V_d and V_q . The reactive power controller is responsible for regulating the voltage at the PCC within the admissible limits while improving the PF. Thus, the controller guides the inverter to absorb or provide reactive power related to the required conditions. It is achieved by generating the required I_q reference to the current controller. The reactive power control is based on the voltage behavior at the PCC and subjected to the inverter limitation. The voltage at the PCC is continuously measured and determined the proper I_q reference relevant to the instantaneous PV power to manage the voltage and improve the PF at the PCC.

2.4. Overall system model

The implemented simulation model of the grid-connected BIPV system is illustrated in Fig. 11. The system module parameters are summarized in Table 2.

3. Results and discussions

This paper is providing more detail extended results of our work reported in ref [36]. In this work, as the first approach model validation is performed with real system data to ensure a better system accuracy of the developed system model. Then, to analyse the effectiveness of the inverter reactive power control, the implemented system is numerically investigated under real data profiles for solar and loading.

3.1. Model validation with results of an operational ZEB system

One of the objectives of this research is to validate the developed MATLAB Simulink model of the grid-connected BIPV system. The

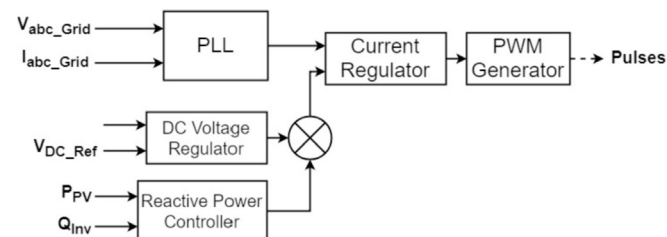


Fig. 10. VSI controller model.

system performance is analyzed utilizing the real solar irradiance and PV cell temperature profiles in two typical days in winter and summer in this regard. The model PV power results are analyzed and compared with the real measured data from an operational ZEB system for model verification. A unity PF (UPF) model without the reactive power control is considered in this process of validation since the ZEB system is a UPF system.

The system is simulated considering the actual solar radiation and cell temperature profiles, which were measured from an installed PV system in a ZEB site, for two typical days in the month of September and January. The typical day in September is a sunny day while in January is a winter day.

The PV power output of the model is compared with the actual PV power measured data from relevant ZEB system for each respective day as illustrated in Fig. 12 and Fig. 13. It can be observed that the PV power output of the model is high in both days compared to the real data.

The Root Mean Squared Error (RMSE) and the total PV energy production comparison for the model and actual system in January and September are summarized in Table 3. The RMSE value indicates the degree of accuracy of the MATLAB model with the actual system. A lower value of RMSE leads to a better fit with the actual system. Theoretically, the model PV power is high due to no losses are considered in modeling when compared with the actual system.

3.2. Voltage regulation with inverter var compensation

Mitigation of the voltage fluctuation at the PCC due to different dynamic loading conditions is investigated by enabling the reactive power compensation of the inverter. Hence, the voltage behavior at the PCC is explored under two inverter operating modes where the reactive power compensation is enabled and disabled conditions, for dynamic lagging and leading PF loading conditions.

The system without inverter reactive power compensation (unity PF system) is simulated separately for both dynamic inductive and capacitive loading conditions at the PCC. The root mean squared (RMS) voltage characteristics at the PCC are indicated in Fig. 14 for the inductive loading condition and Fig. 15 for the capacitive loading condition.

It can be observed that the RMS voltage at the PCC is dropped below 395 V as a consequence of the inductive loading condition while an increment in the RMS voltage is occurred above 405 V due to the effect of the capacitive loading condition at the PCC. The voltage conditions at the PCC are violated in both inductive and capacitive loading conditions.

The behavior of the system with inverter reactive power compensation is investigated for both dynamic inductive and capacitive loading conditions at the PCC. The reactive power control of the inverter is responsible for regulating the RMS voltage at PCC within the range of $\pm 5\%$ of 400 V, regardless of any load conditions at PCC. The RMS voltage characteristics at the PCC are represented in Fig. 16 for the inductive loading condition and Fig. 17 for the capacitive loading condition.

By enabling the inverter reactive power compensation, it can be noticed the RMS voltage at the PCC is continuously maintained at 400 V in both loading conditions without any violations.

3.3. System performance evaluation with real operational data

The system power flow relationship with the sign convention as represented in Fig. 18 is very important fact in the process of system analysing. The general rule for the sign convention is referenced to the inverter operation. If the inverter feeds, the sign is positive and if the inverter consumes, the sign is negative. Based on this, the

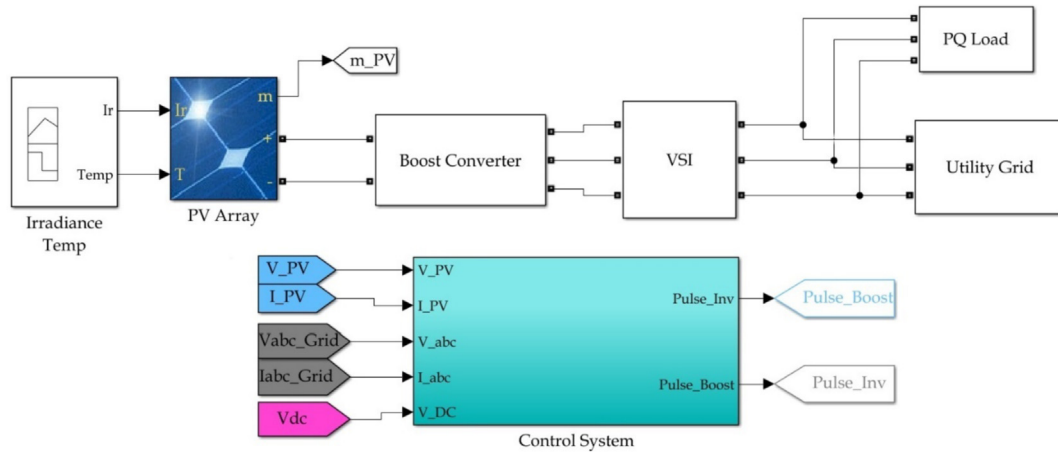


Fig. 11. Simulation model of the three-phase grid-connected BIPV system.

Table 2
System module parameters.

| Parameter | Value |
|-------------------------|-------|
| PV Capacity (kW) | 7.63 |
| Inverter Capacity (kVA) | 9.5 |
| Three Phase Voltage (V) | 400 |
| DC Bus Voltage (V) | 800 |
| Grid Voltage (kV) | 11 |
| Frequency (Hz) | 50 |

Table 3
Comparison of the MATLAB model and the actual system in January and September.

| Month | RMSE | Total Energy Production (kWh) | |
|-----------|--------|-------------------------------|--------|
| | | Model | Actual |
| January | 0.3066 | 470.08 | 393.53 |
| September | 0.3801 | 1031.31 | 916.46 |

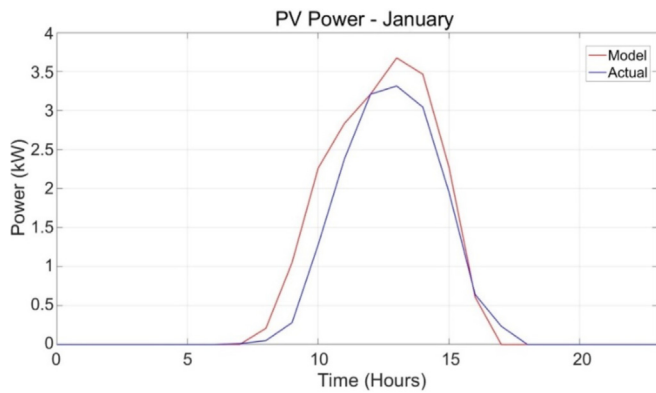


Fig. 12. PV output power comparison between the module and actual system in January.

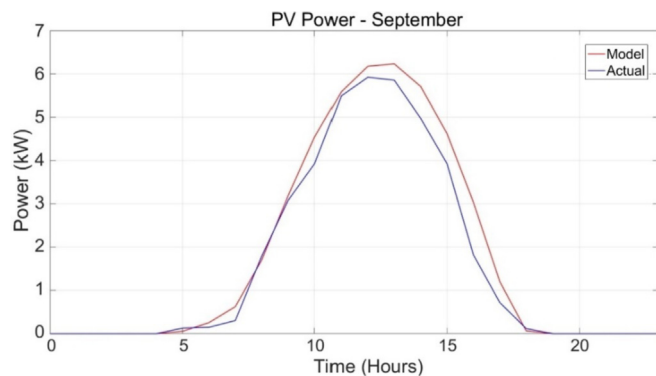


Fig. 13. PV output power comparison between the module and actual system in September.

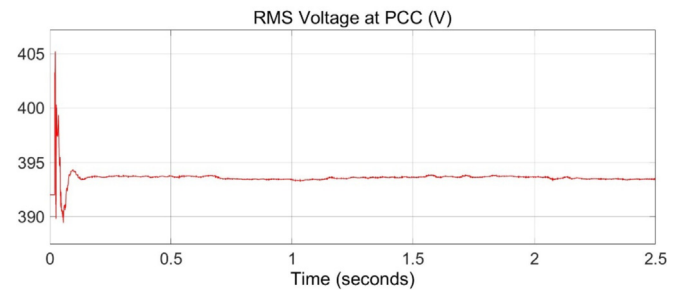


Fig. 14. RMS voltage characteristic at the PCC for the inductive load.

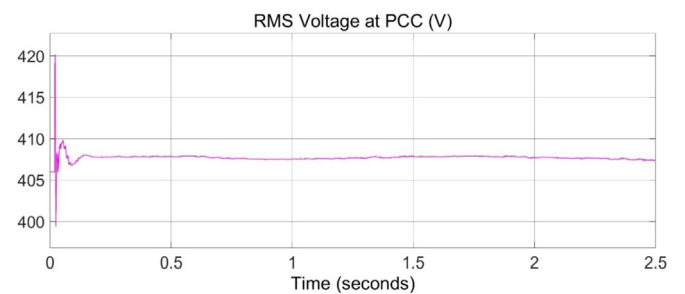


Fig. 15. RMS voltage characteristic at the PCC for the capacitive load.

opposite sign is assigned for injection and consumption for both the grid and the load.

In this study, the actual solar radiation along with the cell temperature data which are measured from a Zero Energy Building (ZEB) system is utilized. The ZEB system's load profile is considered as the dynamic load condition at the PCC, where the load PF varies in the range of 0.8–0.95.

The system is simulated considering the solar radiation and the

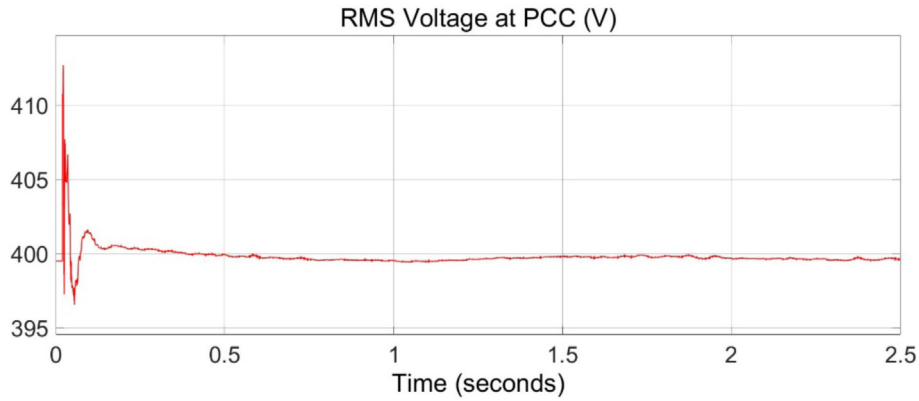


Fig. 16. RMS voltage characteristic at the PCC for the inductive load.

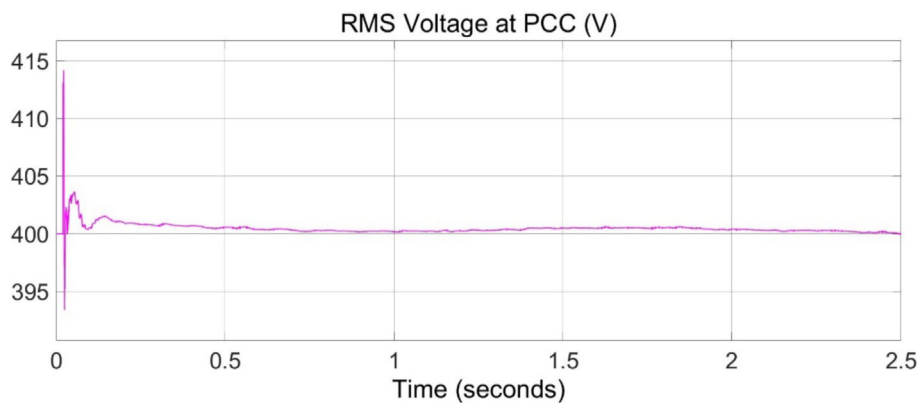


Fig. 17. RMS voltage characteristic at the PCC for the capacitive load.

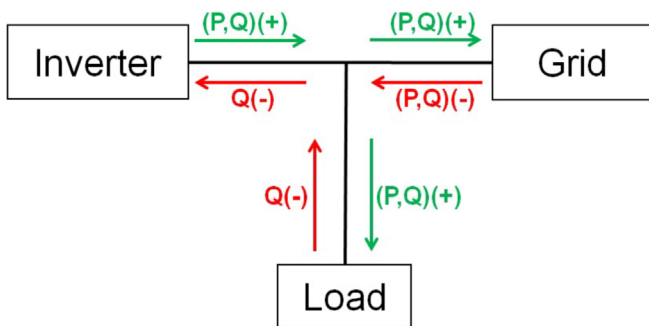


Fig. 18. Relationship of the system power flow characteristic.

cell temperature profiles of the midday in the months of January and June.

3.3.1. System performance evaluation in January

The related load profile of the day is depicted in Fig. 19. The maximum real load of the day is more than 4 kW and the reactive power varies with respect to the load PF. Fig. 20 represents the PV power characteristic of the midday in January. The peak PV power is less than 4 kW.

The inverter power flow characteristic and the PF variation are illustrated in Fig. 21 and Fig. 22 respectively. It can be observed that the inverter var compensation is high when there is no PV power. It gradually decreases with the PV power. The inverter operating PF is in the range of 0–0.4.

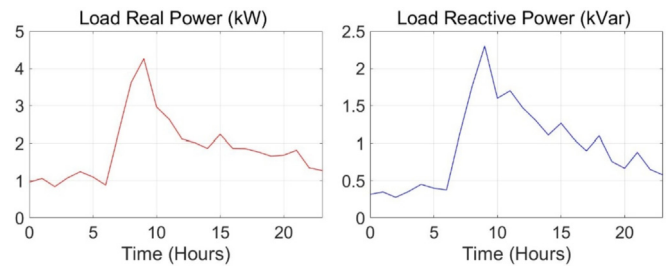


Fig. 19. Load power flow characteristic.

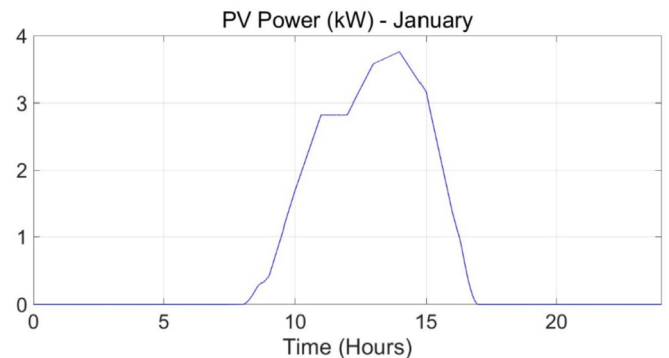


Fig. 20. PV power characteristic.

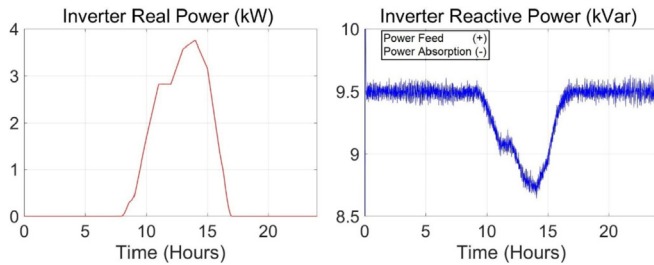


Fig. 21. Inverter power flow characteristic.

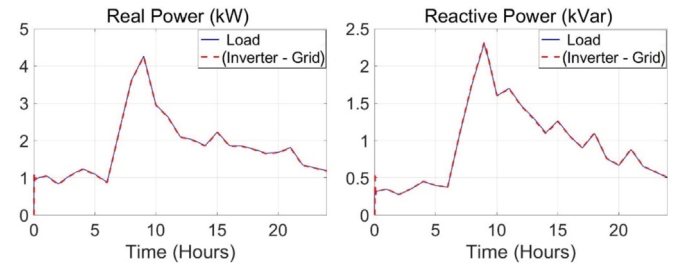


Fig. 24. System power flow characteristic.

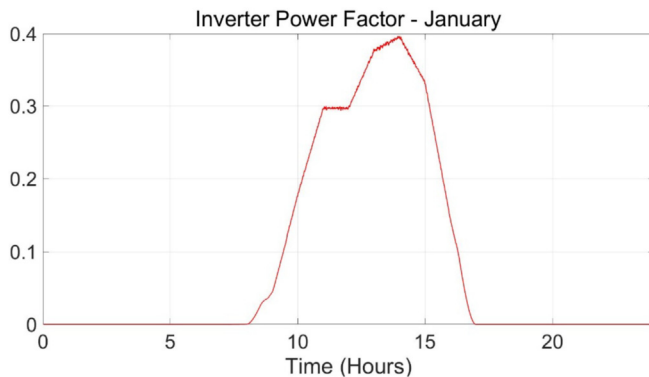


Fig. 22. Inverter PF characteristic.

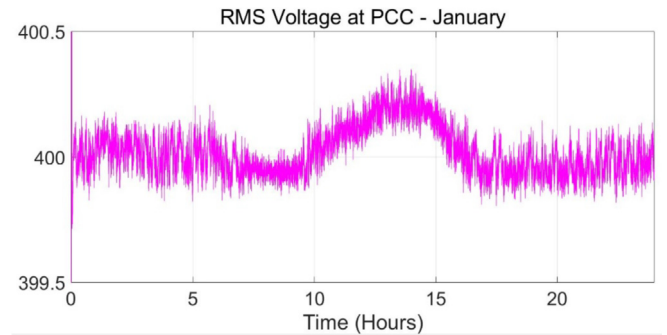


Fig. 25. RMS voltage characteristic at the PCC.

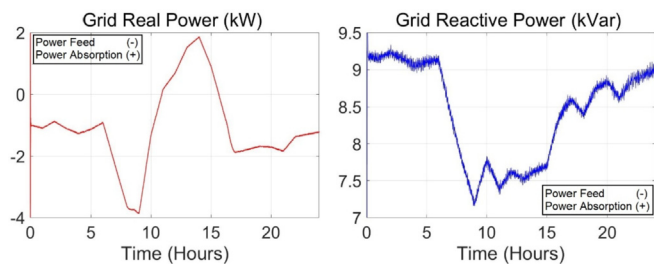


Fig. 23. Grid power flow characteristic.

It is observed that the grid is responsible for serving the load when there is no PV power and absorbs the excess reactive power from the inverter as can be illustrated in Fig. 23. The illustration of the overall system power flow characteristic is given in Fig. 24. The RMS voltage characteristic at the PCC is shown in Fig. 25.

A slight increment is noticed in the RMS voltage when the inverter var compensation is gradually decreasing.

3.3.2. System performance evaluation in June

Generally, June is one of the months in the summer season. The system performance is explored using solar radiation and cell temperature profile of the midday in the month of June. The related load profile of the day is shown in Fig. 26.

The power characteristics of the PV module and the inverter are illustrated in Fig. 27 and Fig. 28 respectively. High PV penetrations can be observed throughout the day. The inverter PF characteristic is shown in Fig. 29. The inverter operates in maximum operating PF during the mid-hours while lowering the inverter var compensation.

The grid power flow characteristic is indicated in Fig. 30. The overall system power flow and the RMS voltage characteristic at the

PCC are represented in Fig. 31 and Fig. 32 respectively.

It can be noticed that the RMS voltage at the PCC escalates above 401 V during the mid-hours of the day when the inverter PF is high. But the overall system manages to operate subject to the limitations.

The simulation result of the overall system performance for real data indicate that the system is ready to feed maximum available power from the PV module and the reactive power subjected to the inverter capacity regardless of any loading conditions to regulate the system voltage and improve the system PF at low or high PV penetration situations where the grid fulfills the load demand when there is no PV power and absorbs excess reactive power from the inverter. This implies that the system functions with its duties where it leads to a better BIPV system operation by reducing the burden on the utility grid.

4. Conclusions

This research work presents an overall implementation of a 3-phase grid connected BIPV system with the reactive power control capability. The system model includes a PV array module with 7.63 kW capacity, a 3-phase VSI with 9.5 kVA capacity, a boost converter, a 3-phase dynamic load and a utility grid. The main aim of this work is to utilize the reactive power ability of the VSI to regulate the system voltage and improve the system PF by enabling the inverter var compensation while reducing the var compensation from the utility grid. The reactive power control is designed and implemented based on the voltage behavior at the PCC with the inverter limitations and embedded into the inverter control system. Hence, the VSI is responsible for regulating and converting the PV DC power to the AC power while producing and absorbing reactive power as an ancillary service. The boost converter ensures the operation of the PV system at MPP.

The validity and the accuracy of the implemented model were verified by comparing the system performance results with a real system. A better system accuracy was demonstrated from the

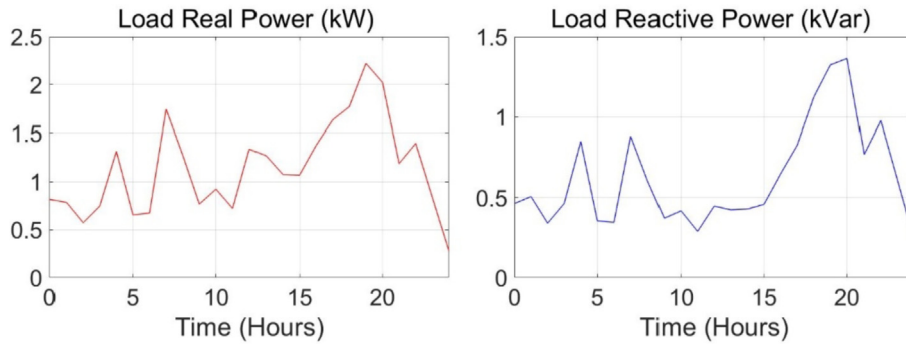


Fig. 26. Load power flow characteristic.

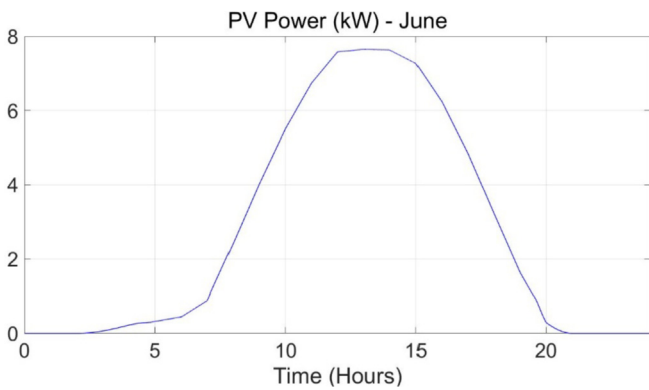


Fig. 27. PV power characteristic.

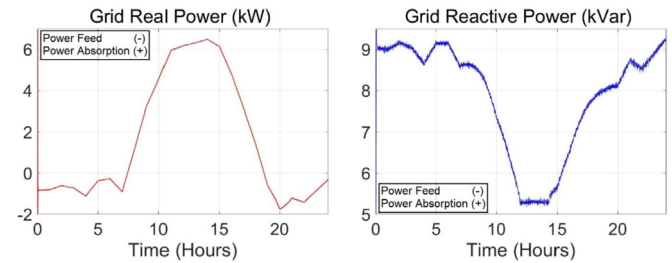


Fig. 30. Grid power flow characteristic.

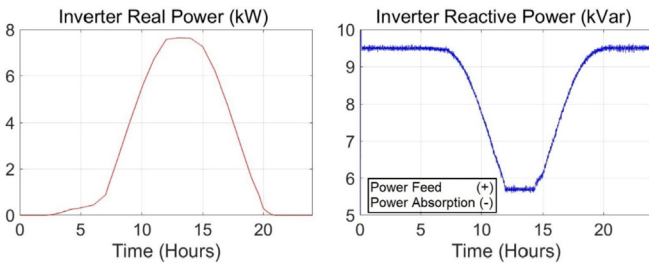


Fig. 28. Inverter power flow characteristic.

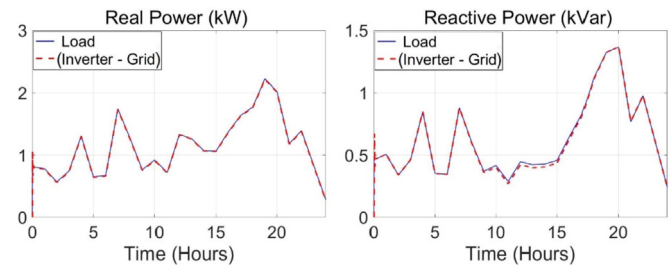


Fig. 31. System power flow characteristic.

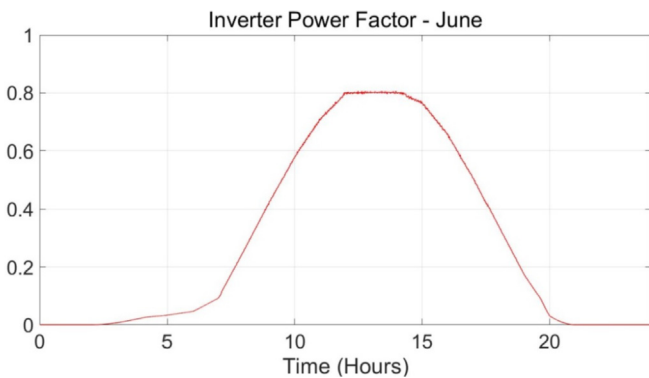


Fig. 29. Inverter PF characteristic.

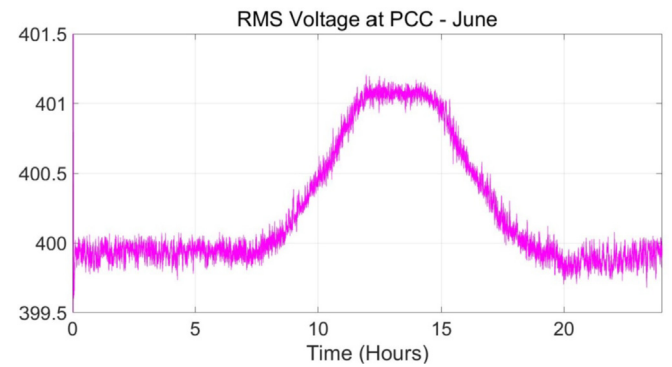


Fig. 32. RMS voltage characteristic at the PCC.

results. Hence, this research study suggests that more focuses on effective utilization of the reactive power capability of a 3-phase

grid-connected BIPV system capitalize on the utility grid to minimize the complexity of the control operation for mitigating the PV system effects on the system network.

Declaration of competing interest

The authors declare that they have no known competing

financial interests or personal relationships that could have appeared to influence the work reported in this paper.

CRediT authorship contribution statement

Mohan Lal Kolhe: Conceptualization, Resources, Supervision, Writing - review & editing, Funding acquisition. **M.J.M.A. Rasul:** Methodology, Software, Validation, Formal analysis, Data curation, Writing - original draft.

Acknowledgement

Funding: This research work was received a partial support of the Research Council of Norway and partners (Agder Energy Nett AS, Teknova AS, Eltek AS) in the project "Electricity Usage in Smart Village Skarpnes"(Project no. NFR-226139). This work was also partially supported by the Norwegian Ministry of Foreign Affairs under the framework agreement with the TERI (India) and University of Agder (Norway) for project theme "Sustainability and Clean Energy".

References

- [1] International energy agency photovoltaic power systems programme [Online], <http://www.iea-pvps.org>, 2017. Accessed: 15- Apr- 2018.
- [2] R. Tonkoski, L.A.C. Lopes, Voltage regulation in radial distribution feeders with high penetration of photovoltaic, Proc. IEEE Energy 2030 Conf. (2008) 1–7.
- [3] Y. Ueda, T. Oozeki, K. Kurokawa, T. Itou, K. Kitamura, Y. Miyamoto, M. Yokota, H. Sugihara, S. Nishikawa, Analytical results of output restriction due to the voltage increasing of power distribution line in grid-connected clustered PV systems, Conf. Rec. 31st IEEE Photovoltaic Specialists (2005) 1631–1634.
- [4] Y. Ueda, K. Kurokawa, T. Tanabe, K. Kitamura, H. Sugihara, Analysis results of output power loss due to the grid voltage rise in grid-connected photovoltaic power generation systems, IEEE Trans. Ind. Electron. 55 (7) (2008) 2744–2751.
- [5] P. Jahangiri, D. Aliprantis, Distributed volt/VAR control by PV inverters, IEEE Trans. Power Syst. 28 (3) (2013) 3429–3439.
- [6] C. Chang, Y. Lin, Y. Chen, Y. Chang, Simplified reactive power control for single-phase grid-connected photovoltaic inverters, IEEE Trans. Ind. Electron. 61 (5) (2014) 2286–2296.
- [7] W. Peng, Y. Baghzouz, S. Haddad, Local load power factor correction by a grid-interactive PV inverter, in: IEEE-PowerTech, Grenoble, France., June, 2013.
- [8] IEEE Std. 1547-2003, IEEE Standard for Interconnecting Distributed Resources with Electric Power Systems, IEEE, 2003.
- [9] IEEE Std. 1547a-2014, IEEE Standard for Interconnecting Distributed Resources with Electric Power Systems - Amendment 1, IEEE, 2014.
- [10] T. Fawzy, D. Premm, B. Bletterie, A. Gorsek, Active contribution of PV inverters to voltage control - from a smart grid vision to fullscale implementation, Elektrotechnik und Informationstechnik 128 (2011) 110–115.
- [11] A.M. Howlader, S. Sadoyama, L.R. Roose, S. Sepasi, Distributed voltage regulation using Volt-Var controls of a smart PV inverter in a smart grid: an experimental study, Renew. Energy 127 (2018) 145–157.
- [12] VDE-AR-N 4105:2011-08 Forum Netztechnik/Netzbetrieb im VDE (FNN), 2011. Power Generation Systems Connected to the Low/Voltage Distribution Network.
- [13] R. Tonkoski, L.A. Lopes, Impact of active power curtailment on overvoltage prevention and energy production of PV inverters connected to low voltage residential feeders, Renew. Energy 36 (12) (2011) 3566–3574.
- [14] L. Collins, J. Ward, Real and reactive power control of distributed PV inverters for overvoltage prevention and increased renewable generation hosting capacity, Renew. Energy 81 (2015) 464–471.
- [15] M. Ghasemi, M. Parniani, Prevention of distribution network overvoltage by adaptive droop-based active and reactive power control of PV systems, Elec. Power Syst. Res. 133 (2016) 313–327.
- [16] G. Nguyen, K. Uchida, Active and reactive power control techniques based on feedback linearization and fuzzy logic for three-phase grid connected photovoltaic inverters, Asian J. Contr. 17 (5) (2014) 1522–1546.
- [17] S. Ozdemir, S. Bayhan, I. Sefa, N. Altin, Three-phase multilevel grid interactive inverter for pv systems with reactive power support capability, in: Smart Grid and Renewable Energy (SGRE) 2015 First Workshop on, 2015, pp. 1–6.
- [18] G. Kerber, R. Witzmann, H. Sappl, Voltage limitation by autonomous reactive power control of grid connected photovoltaic inverters, Proc. Int. Conf. C. Power Electron. (2009) 129–133.
- [19] B. Bletterie, A. Gorsek, T. Fawzy, D. Premm, W. Deprez, F. Truyenes, A. Woyte, B. Blazic, B. Uljanic, Development of innovative voltage control for distribution networks with high photovoltaic penetration: voltage control in high PV penetration networks, Prog. Photovoltaics Res. Appl. 20 (6) (Sep. 2012) 747–759.
- [20] Y. Yang, H. Wang, F. Blaabjerg, M. Simes, Power control exibilities for grid-connected multi-functional photovoltaic inverters, IET Renew. Power Gener. 10 (4) (2016) 504–513.
- [21] G. Tsengenes, G. Adamidis, Investigation of the behavior of a three phase grid-connected photovoltaic system to control active and reactive power, Elec. Power Syst. Res. 81 (1) (2011) 177–184.
- [22] E. Demirok, P. Gonzalez, K. Frederiksen, D. Sera, P. Rodriguez, R. Teodorescu, Local reactive power control methods for overvoltage prevention of distributed solar inverters in low-voltage grids, IEEE J. Photovoltaics 1 (2) (2011) 174–182.
- [23] R. Aghatehrani, A. Golnas, Reactive power control of photovoltaic systems based on the voltage sensitivity analysis, in: Proc. IEEE PES Gen. Meet, 2012, pp. 1–5.
- [24] M. Farivar, R. Neal, C. Clarke, S. Low, Optimal inverter VAR control in distribution systems with high PV penetration, in: Proc. IEEE PES General Meet, 2012, pp. 1–7.
- [25] C. Garcia Bajo, S. Hashemi, S.B. Kjsar, Guangya Yang, J. stergaard, Voltage unbalance mitigation in LV networks using three-phase PV systems, in: Industrial Technology (ICIT) 2015 IEEE International Conference on, 2015, pp. 2875–2879, 17–19 March.
- [26] A. Samadi, R. Eriksson, L. Soder, B. Rawn, J. Boemer, Coordinated active power-dependent voltage regulation in distribution grids with PV systems, IEEE Trans. Power Deliv. 29 (3) (2014) 1454–1464.
- [27] K. Turitsyn, P. Sulc, S. Backhaus, M. Chertkov, Distributed control of reactive power flow in a radial distribution circuit with high photovoltaic penetration, Proc. IEEE Power Energy Soc. Gen. Meet. (2010-Jul) 1–6.
- [28] E. Dall'Anese, S. Dhople, G. Giannakis, Optimal dispatch of photovoltaic inverters in residential distribution systems, IEEE Trans. Sustain. Energy 5 (2) (2014) 487–497.
- [29] X. Su, M. Masoum, P. Wolfs, Optimal PV inverter reactive power control and real power curtailment to improve performance of unbalanced four-wire LV distribution networks, IEEE Trans. Sustain. Energy 5 (3) (2014) 967–977.
- [30] S. Ghosh, S. Rahman, M. Pipattanasomporn, Local distribution voltage control by reactive power injection from PV inverters enhanced with active power curtailment, in: 2014 IEEE PES General Meeting, 2014, pp. 1–5.
- [31] F. Balaabjerg, R. Teodorescu, Z. Chen, M. Liserre, Power converters and control of renewable energy systems, in: Proc. 6th Int. Conf. Power Electron, 2004 pp.1–20.
- [32] H. Haeberlin, Evolution of inverters for grid connected PV-systems from 1989 to 2000, in: Proc. 17th Eur. Photovoltaic Solar Energy Conf., Munich, Germany, Oct. 22–26, 2001, pp. 426–430.
- [33] J.M. Carrasco, et al., Power-electronic systems for the grid integration of renewable energy sources: a survey, IEEE Trans. Ind. Electron. 53 (4) (Jun. 2006) 1002–1016.
- [34] S. Sumathi, A.L. Kumar, P. Surekha, Solar PV and Wind Energy Conversion Systems: an Introduction to Theory, Modeling with Matlab/Simulink, and the Role of Soft Computing Techniques, Springer International Publishing AG, Switzerland, 2015.
- [35] T. Esmar, P.L. Chapman, Comparison of Photovoltaic array maximum power point tracking techniques, IEEE Trans. Energy Convers. 22 (2) (Jun. 2007) 439–449.
- [36] M.J.M.A. Rasul, Mohan Kolhe, Reactive power control of a 3-phase grid-connected building integrated photovoltaic system, in: 5th International Symposium on Hydrogen Energy, Renewable Energy and Materials (HEREM 2019), IOP Conference Series: Materials Science and Engineering (MSE), 2019 (accepted, in press).